DOI: 10.3901/CJME.2013.04.689, available online at www.springerlink.com; www.cjmenet.com; www.cjmenet.com.cn

Development of a Miniature Permanent Magnetic Circuit for Nuclear Magnetic Resonance Chip

LU Rongsheng, YI Hong, WU Weiping, and NI Zhonghua*

Jiangsu Key Laboratory for Design and Manufacture of Micro-Nano Biomedical Instruments, Southeast University, Nanjing 211189, China

Received September 14, 2012; revised March 7, 2013; accepted April 18, 2013

Abstract: The existing researches of miniature magnetic circuits focus on the single-sided permanent magnetic circuits and the Halbach permanent magnetic circuits. In the single-sided permanent magnetic circuits, the magnetic flux density is always very low in the work region. In the Halbach permanent magnetic circuits, there are always great difficulties in the manufacturing and assembly process. The static magnetic flux density required for nuclear magnetic resonance(NMR) chip is analyzed based on the signal noise ratio(SNR) calculation model, and then a miniature C-shaped permanent magnetic circuit is designed as the required magnetic flux density. Based on Kirchhoff's law and magnetic flux refraction principle, the concept of a single shimming ring is proposed to improve the performance of the designed magnetic circuit. Using the finite element method, a comparative calculation is conducted. The calculation results demonstrate that the magnetic circuit improved with a single shimming has higher magnetic flux density and better magnetic field homogeneity than the one improved with no shimming ring or double shimming rings. The proposed magnetic circuit is manufactured and its experimental test platform is also built. The magnetic flux density measured in the work region is 0.7 T, which is well coincided with the theoretical design. The spatial variation of the magnetic field is within the range of the instrument error. At last, the temperature dependence of the magnetic flux density produced by the proposed magnetic circuit is investigated through both theoretical analysis and experimental study, and a linear functional model is obtained. The proposed research is crucial for solving the problem in the application of NMR-chip under different environmental temperatures.

Key words: nuclear magnetic resonance, microfluidic chip, permanent magnet, magnetic flux density

1 Introduction

Though they are the most widely used techniques for the analysis of microfluidic devices, optical detection[1] and electrochemical detection[2] suffer from serious limitations that restrict the commercialization of the microfluidic chips[3]. The optical methods need for optical access to the region of interest which necessarily limits the range of materials that can be used for device fabrication[4], and the electrochemical methods may destruct the living samples. As a probative detection technique, nuclear magnetic resonance(NMR) can bypass some of these limitations because of its nondestructiveness and versatility[4]. Integration with microstructure devices, the concept of nuclear magnetic resonance chip(NMR-chip)[5] has been proposed.

NMR-chip has been successfully used in detecting microfluidic specimen[6]. However, a probative miniature magnetic circuit is very important for the commercialization of this concept. Permanent magnetic circuits with simple structure, low cost, small size and no extra energy will be optimal for portable nuclear magnetic resonance, especially for NMR-chip. Most researches on portable permanent magnetic circuit are focused on single-sided permanent magnetic circuits, which produce inhomogeneous[7–8] or homogenous[9–10] magnetic field above the whole magnetic circuit as the detection region. Although NMR with single-sided permanent magnetic circuit is advantageous in detecting arbitrarily-sized samples, its magnetic flux density is relatively low. Halbach permanent magnetic circuits[11] can produce high magnetic flux density with their sizes being smaller than any other permanent magnetic circuits. However, Halbach permanent magnetic circuit is commonly a circular structure composed of several permanent magnet blocks, which needs much adjustment till the expected results are obtained[11–12]. Therefore, the performance of the magnetic circuit will be greatly limited by the manufacture and assembly precision. In most cases, extra shimming coils are needed to improve the magnetic field homogeneity[13].

As the third generation permanent magnet material, NdFeB has higher remanent field and energy density, and is

* Corresponding author. E-mail: nzh2003@seu.edu.cn

This project is supported by National Natural Science Foundation of China (Grant No. 51175083), Jiangsu Provincial University Industry Cooperation Innovation Foundation-Prospective Study of China (Grant No. BY2011135), Scientific Research Foundation of Graduate School of Southeast University, China (Grant No. YBJJ1134), and Important Scientific Research Guide Foundation of Southeast University, China

more inexpensive than other permanent magnet materials. Therefore, in this paper, based on the theoretical analysis of NMR-chip for achieving the required magnetic flux density, a miniature C-shaped permanent magnetic circuit using NdFeB was studied from aspects of theoretical design and its performance improvement, simulation, and experimental verification. Considering that NdFeB permanent magnet has large temperature coefficient, the performance of the designed magnetic circuit will vary with temperature variation. Therefore, the temperature dependence of the magnetic flux density produced by the proposed magnetic circuit was investigated through both theoretical analysis and experimental study.

2 Theoretical Analysis of Design Object

Nuclear magnetic resonance is a spectroscopic technology based on the interaction of the magnetic nuclear placed in an external magnetic field with an applied electromagnetic field oscillating at a particular frequency[14]. Therefore, the NMR signal is regarded as an induction current produced by magnetic nuclear cutting magnetic flux, and the signal noise ratio(SNR) r_{snr} reflects the sensitivity of the NMR devices. The theoretical calculation model of r_{snr} [15] is shown as follows:

$$r_{\mathrm{snr}}=\frac{K(B_1)_{xy}V_{\mathrm{s}}N\gamma\hbar^2I(I+1)}{7.12kT_{\mathrm{s}}}\cdot\left(\frac{p}{FkT_{\mathrm{c}}l\zeta\Delta f}\right)^{1/2}\cdot\frac{{\omega_0}^{7/4}}{\left[\mu\rho(T_{\mathrm{c}})\right]^{1/4}}=\frac{K(B_1)_{xy}V_{\mathrm{s}}N\gamma^{11/4}\hbar^2I(I+1)}{7.12kT_{\mathrm{s}}}\cdot\left(\frac{p}{FkT_{\mathrm{c}}l\zeta\Delta f}\right)^{1/2}\cdot\frac{1}{\left[\mu\mu_0\rho(T_{\mathrm{c}})\right]^{1/4}}\cdot{B_0}^{7/4},\tag{1}$$

where $K(B_1)_{xy}$ is the effective field over the sample volume produced by the unit current flowing in the receiving coil, V_{s} is the sample volume, I is the spin quantum number of the magnetic nuclear, N is the spin density, γ is the magnetogyric ratio, k is Boltzmann's constant, $\hbar=h/2\pi$ (h is the planck constant), T_{s} is the sample temperature, p is the perimeter of the radio frequency (RF coil), l is the length of the RF coil, F is the noise figure of the preamplifier, ζ is the proximity factor, T_{c} is the temperature of the RF coil, Δf is the bandwidth of the receiver, $\rho(T_{\mathrm{c}})$ is the resistivity of the RF coil, μ is the permeability of the RF coil, and B_0 is the static magnetic flux density, and μ_0 is the permeability of vacuum.

As shown in Eq. (1), r_{snr} is related to the value of B_0, the property of the RF coil, the property of the sample, and the detection condition. Therefore, assuming that C is a constant decided by the property of the RF coil, the property of the sample and the detection condition (ignoring the effect of magnetic field inhomogeneity), Eq. (1) can be deduced as

$$\frac{r_{\mathrm{snr}_1}}{r_{\mathrm{snr}_2}}=\frac{C_1}{C_2}\cdot\frac{{B_0}_1^{7/4}}{{B_0}_2^{7/4}}.\tag{2}$$

In attempts to effectively use NMR technologies for detecting samples, SNR must be no less than 3[16]. SNR reaching 550 has been achieved using a micro-RF coil in 1.5 T static magnetic flux density condition[17]. Therefore, when the same micro-RF coil is used in NMR-chip to detect the same sample and the detection condition is assumed to be consistent, in order to ensure the SNR is greater than 3, the calculated minimum static magnetic flux density B_0 in the detection region must be greater than 0.07 T based on Eq. (2). However, in this paper the magnetic flux density B_0 in the detection region of the magnetic circuit is set at 0.7 T to guarantee the sensitivity and resolution of the NMR-chip.

3 Miniature Magnetic Circuit Design

C-shaped permanent magnetic circuit can be easily manufactured and assembled, so it is adopted here for the NMR-chip magnetic circuit design. The miniature magnetic circuit is composed of two permanent magnet blocks, some magnetizer blocks, two shimming sheets and an air gap, as shown in Fig. 1(a) (The arrows represent the magnetization direction of the permanent magnet blocks), Fig. 1(b) describes the distribution of the magnetic induction line of the magnetic circuit shown in Fig. 1(a). NdFeB N_{52} with remanence B_{r} of about 1.477 5 T and coercivity H_{cj} of about 916.7 kA/m was chosen as the material of the permanent magnet blocks (the demagnetization curve of NdFeB N52 is shown in Fig. 2), and electrical pure iron DT_4 was chosen as the material of magnetizer blocks and shimming sheets. Based on Kirchhoff's first and second law, there are two important equations which can be used in permanent magnetic circuit design[18]:

$$S_{\mathrm{m}}=k_{\mathrm{f}}\frac{B_{\mathrm{g}}S_{\mathrm{g}}}{B_{\mathrm{m}}},\tag{3}$$

$$L_{\mathrm{m}}=k_{\mathrm{r}}\frac{H_{\mathrm{g}}L_{\mathrm{g}}}{H_{\mathrm{m}}},\quad H_{\mathrm{g}}=\frac{1}{\mu_0}B_{\mathrm{g}},\tag{4}$$

where S_{m} and L_{m} are the cross-section and the length of the permanent magnet block, S_{g} and L_{g} are the cross-section and the length of the air gap, B_{g} and H_{g} are the magnetic field density and the magnetic field strength in the permanent magnet, k_{r} and k_{f} are respectively the magnetic-leakage coefficient and the magnetic-reluctance coefficient.

Because leakage always exists in any magnetic circuit, for C-shaped permanent magnetic circuit, there exists the correlation in the magnetic circuit design variables[19]:

$$S_{\mathrm{g}}=\left(\sqrt{S_{\mathrm{m}}}+a\frac{L_{\mathrm{g}}}{\pi}\right)^2,\tag{5}$$

where a is a constant related to the ratio of the length of the permanent magnet block and the length of the air gap.

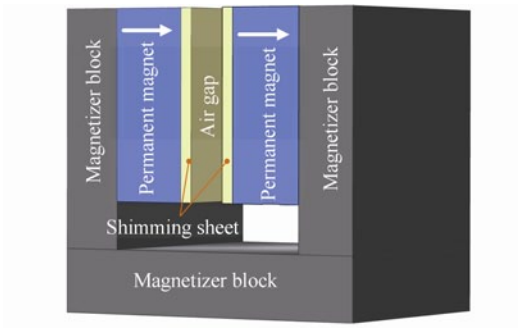

(a) Geometry model of the primary miniature magnetic circuit

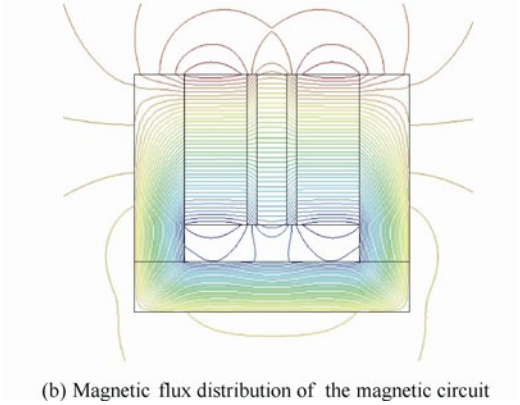

(b) Magnetic flux distribution of the magnetic circuit

Fig. 1. Primary miniature permanent magnetic circuit

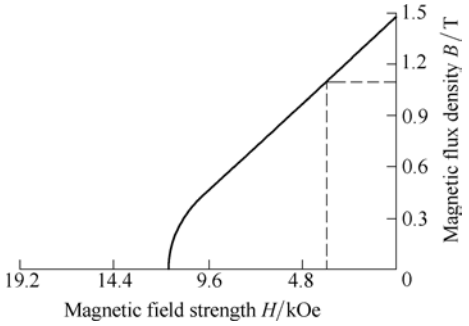

Fig. 2. Demagnetization curve of NdFeB N_{52} (provided by Ningbo Newland Magnetics Co., Ltd.)

According to the former theoretical analysis of the required static magnetic flux density as well as the NMR-chip application, the static magnetic flux density B_g in the air gap was set to 0.7 T, and the length L_g of the air gap was set to 12 mm, and B=1.1 T, H=3.37 kOe in the demagnetization curve (as shown in Fig. 2) are chosen as the working point of the permanent magnet blocks. The values of k_r, k_f and a are respectively set at 1.5, 2.0, and 0.45. Therefore, by combining Eqs. (3)–(5), L_m and S_m can be calculated and their values are respectively 49.8 mm and 4 844.7 mm^2. The magnetic circuit has two identical permanent magnet blocks, so the whole size of the permanent magnet block is 25 mm×80 mm×60 mm.

Similar to sound wave or light wave refraction, magnetic flux will also refract when transmitting through two different mediums with different permeabilities, and the tangent ratio of the angles between each magnetic flux and normal of each mediums is equal to the permeability ratio of the two mediums. The permeability of the permanent magnet block is near vacuum but far lower than the magnetizer block, so magnetic flux in the air gap can easily spread to the surrounding structure, resulting in great magnetic leakage, as shown in Fig. 1(b). This will greatly influence the static magnetic flux density and static magnetic field homogeneity. In conventional methods, a shimming ring is placed on each shimming sheet to reduce the magnetic leakage. However, according to the principle of magnetic flux refraction, the magnetic leakage is mainly caused by the refraction of the magnetic flux when it transmits from the shimming sheet to the air gap. Therefore, only the left shimming sheet requires a shimming ring, that is, only single shimming ring is needed for the miniature C-shaped permanent magnetic circuit improvement. The final improved permanent magnetic circuit was designed as shown in Fig. 3.

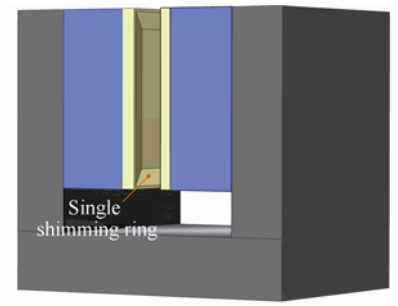

(a) Diagram of improved magnetic circuit

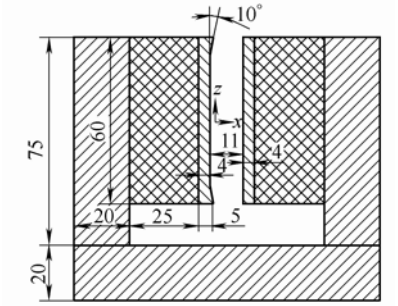

(b) Dimensional size of the improved magnetic circuit shown (x-z sectional view)

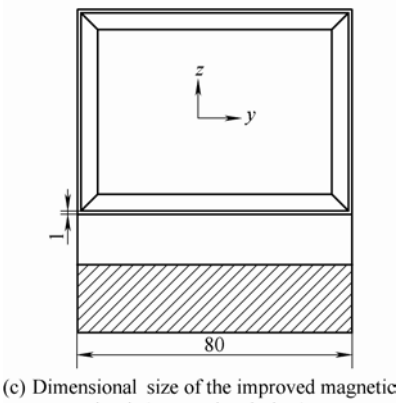

(c) Dimensional size of the improved magnetic circuit (z-y sectional view)

Fig. 3. Miniature C-shaped permanent magnetic circuit improved with a single shimming ring

4 Simulation and Analysis

The correlation between the permanent magnetic circuit and design variables has high nonlinear characteristics. It can hardly be expressed by an explicit formulation like the Kirchhoff's laws which can only be used as primary estimate. Therefore, the finite element method (Ansoft Maxwell) was used here to calculate the design permanent magnetic circuit. When using finite element method, the default balloon boundary condition of Ansoft Maxwell is selected. Three differently improved magnetic circuits with no shimming ring, double shimming rings and a single shimming ring respectively were compared. Fig. 4 depicts the calculated nephograms of their magnetic flux density distribution, showing it is obvious that the permanent magnetic circuit improved with single shimming ring has less magnetic leakage and higher magnetic flux density in the air gap.

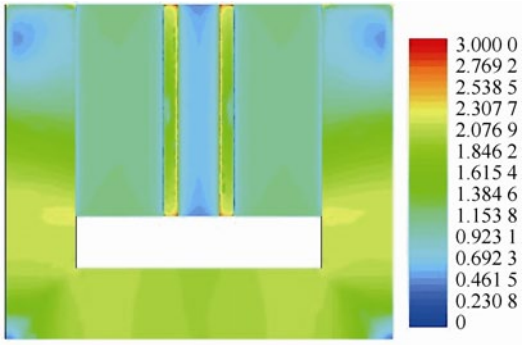

(a) Magnetic circuit improved with no shimming ring

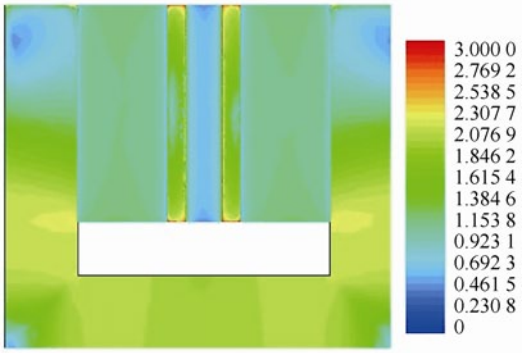

(b) Magnetic circuit improved with double shimming rings

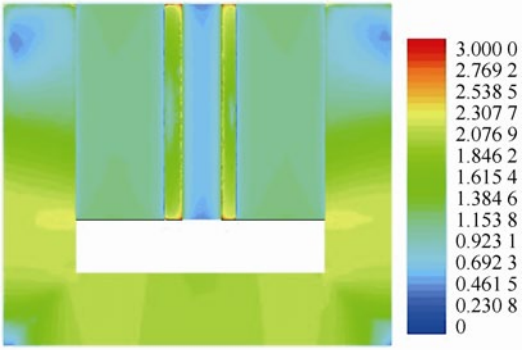

(c) Magnetic circuit improved with a single shimming ring

Fig. 4. Nephograms of magnetic flux density distribution from three different improved permanent magnetic circuits (T)

Table 1 lists the calculated values of the average magnetic flux density B_a and the magnetic field homogeneity P in the 1 mm×1 mm×1mm detection region of the three different magnetic circuits. While the magnetic circuit improved with traditional double shimming rings has less magnetic leakage and a little higher magnetic flux density than the magnetic circuit improved with a single shimming ring, its magnetic field homogeneity is far less than that of the latter. In conclusion, the proposed permanent magnetic circuit improvement has better performance.

Table 1. Calculation values of three differently improved permanent magnetic circuits

Magnetic circuits	Average magnetic flux density B_a/T	Magnetic field homogeneity $P/10^{-6}$
No shimming ring	0.697 429	64
Double shimming rings	0.714 579	1 525
Single shimming ring	0.710 109	40

5 Experiment of the Designed Magnetic Circuit

According to the theoretical results, the miniature permanent magnetic circuit was manufactured and assembled, as shown in Fig. 5. In the manufactured magnetic circuit, the height, width and length of the permanent magnet block are respectively 60 mm, 25 mm, and 80 mm. A test platform used for the permanent magnetic circuit experiment was also built, which is composed of a gaussmeter, a hall probe, a micro-motion stage, a lifting platform and a PC, as shown in Fig. 6.

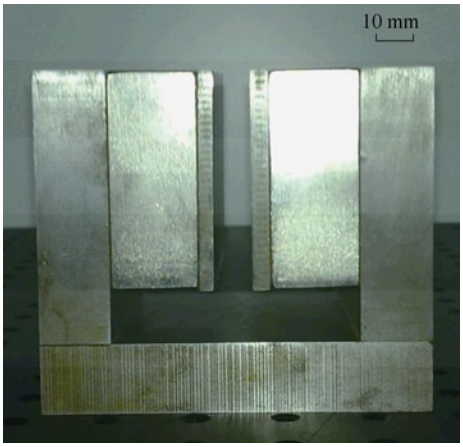

Fig. 5. Manufactured permanent magnetic circuit

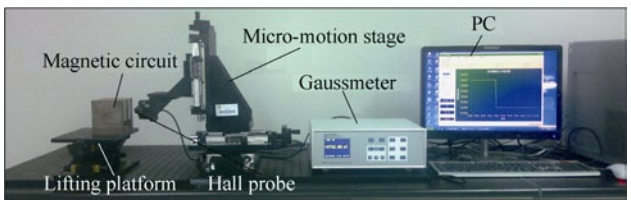

Fig. 6. Test platform used for NMR-chip magnetic circuit measuring

The accuracy of the gaussmeter (CH-1800, CH-HALL Electronic Devices Co., Ltd.) is ±0.05%, and thus, the reading data in the range from 1.000 5% to 0.999 5% should all be regarded as experimental data. Fig. 7(a) shows the distribution of the magnetic flux density in the detection region along coordinates of x, y, and z directions (a_x is the reading data along the coordinate of x from the gaussmeter, a_{x-} is 0.999 5% of the reading data, a_{x+} is 1.000 5% of the reading data, and a_y, a_{y+}, a_{y-}, a_z, a_{z+} and a_{z-} refer to the same value). As is shown in this figure, the spatial variation of the magnetic flux density is in the range of the instrument error, which demonstrates that the manufactured magnetic circuit has perfect magnetic field homogeneity. Fig. 7(b) depicts the contour map of magnetic flux density distribution in x-z plane section of the detection region, showing the magnetic flux density is well coincided with the calculated results shown in Table 1. However, the magnetic field homogeneity is relatively poor compared with the theoretically calculated results, especially along x and y coordinate direction, for which there may be two reasons. One is that it is unable to magnetize the permanent magnet blocks to be completely uniform, and the other is that the poor tolerance precision during the manufacturing and assembling process (because only wire-electrode cutting was used in the machining process without any extra, precision machining), especially the large flatness error and perpendicularity error of the two shimming sheets, greatly influences the magnetic flux density distribution along y and z coordinate direction.

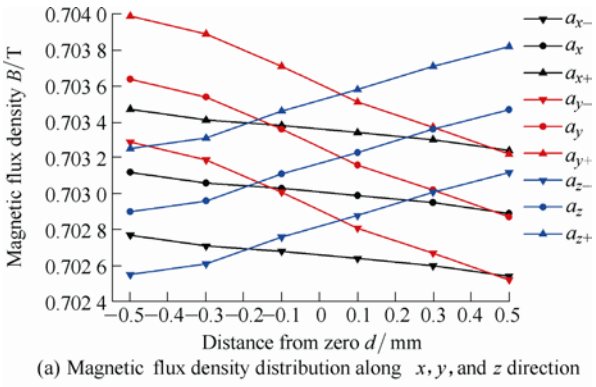

(a) Magnetic flux density distribution along x, y, and z direction

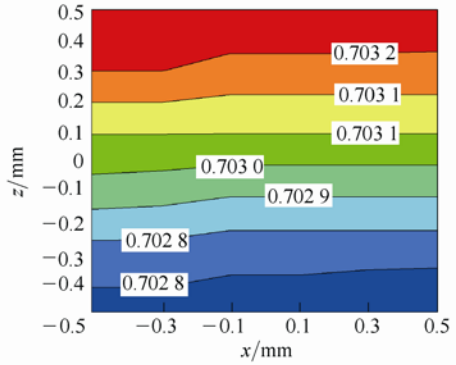

(b) Contour map of magnetic flux density distribution in x-z plane

Fig. 7. Experimental results of the designed magnetic circuit

6 Temperature Dependence of the Designed Magnetic Circuit

As the NdFeB permanent magnet has large temperature coefficient, the performance of the magnetic circuit will change with the temperature variation. As seasonal variation, the NMR-chip will work in the environment from 10 ℃ to 30 ℃, and therefore, the temperature dependence of magnetic flux density produced the permanent magnetic circuit in 10–30 ℃ was studied by both theoretical calculation and experimental method. In the theoretical calculation, the temperature coefficients of the remanence B_r and coercivity H_{cj} are −0.12% and −0.85%, respectively, ignoring the temperature coefficient of the electrical pure iron DT_4. Fig. 8(a) shows the calculated results of the magnetic flux density change in the detection region of the above designed magnetic circuit with the temperature varying from 10 ℃ to 30 ℃. As is shown in this figure, there exists a strictly linear correlation between the magnetic flux density and the temperature. Fig. 8(b) shows the experimental data of the magnetic flux density change in the detection region of the above manufactured magnetic circuit with the temperature varying from 10 ℃ to 30 ℃, a functional model between magnetic flux density B and temperature T is achieved by fitting the experiment data. The functional model is as follows:

$$B = p + mT, T \in [10\ ℃,\ 30\ ℃], \tag{6}$$

where both p and m are constants related to the structure and materials of the magnetic circuit.

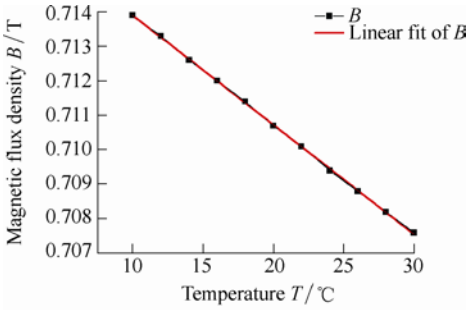

(a) Theoretical calculated results

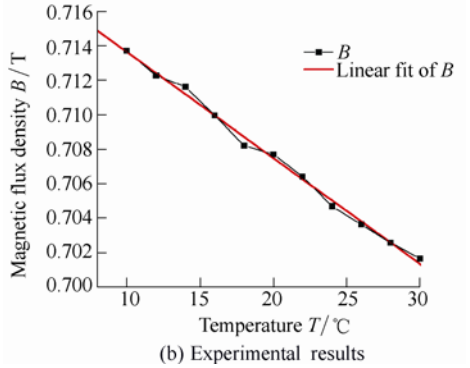

(b) Experimental results

Fig. 8. Relation between magnetic flux density and temperature

As shown in Fig. 8 and Eq. (6), theoretically calculated results and experimental results both demonstrate the relation between magnetic flux density B and temperature T is linear. However, the slopes are different between theoretical calculation and experimental data fitting with the error percentage approaching 48%, which is mainly caused by the theoretical calculation error from ignoring the temperature coefficient of the electrical pure iron DT4, as well as the temperature coefficient errors of the remanence B_r and coercivity H_{cj}.

7 Conclusions

(1) Compared with double shimming rings, a single shimming ring can better improve the performance of the miniature C-shaped permanent magnetic circuit.

(2) The designed miniature magnetic circuit is manufactured, and experimental results show its good performance.

(3) A linear functional model is obtained, which illustrates the relation between the magnetic flux density of the designed permanent magnetic circuit and the environmental temperature. This model is very important for solving the problem arising from the application of NMR-chip under different environmental temperatures.

References

[1] MOGENSEN K B, KLANK H, KUTTER J P. Recent developments in detection for microfluidic systems[J]. *Electrophoresis*, 2004, 25(21–22): 3 498–3 512.

[2] VANDAVEER W R, PASS-FARMER S A, FISCHER D J, et al. Recent developments in electrochemical detection for microchip capillary electrophoresis[J]. *Electrophoresis*, 2004, 25(21–22): 3 528–3 549.

[3] WHITESIDES G M. The origins and the future of microfluidics[J]. *Nature*, 2006, 442(7101): 368–373.

[4] HAREL E. Magnetic resonance detection: spectroscopy and imaging of lab-on-a-chip[J]. *Lab on a Chip*, 2009, 9(3): 17–23.

[5] LEE H, SUN E, HAM D, et al. Chip-NMR biosensor for detection and molecular analysis of cells[J]. *Nature Medicine*, 2008, 14(8): 869–874.

[6] HAUN J B, CASTRO C M, WANG R, et al. Micro-NMR for rapid molecular analysis of human tumor samples[J]. *Science Transl. Med.*, 2011, 3(71): 71ra16.

[7] EIDMANN G, SAVELSBERG R, BLÜMLER P, et al. The NMR MOUSE, a mobile universal surface explorer[J]. *Journal of Magnetic Resonance*, 1996, 122(1): 104–109.

[8] PERLO J, DEMAS V, CASANOVA F, et al. High-resolution NMR spectroscopy with a portable single-sided sensor[J]. *Science*, 2005, 308(5726): 1 279–1 279.

[9] PERLO J, CASANOVA F, BLUMICH B. Ex situ NMR in highly homogeneous fields: H-1 spectroscopy[J]. *Science*, 2007, 315(5815): 1 110–1 112.

[10] MARBLE A E, MASTIKHIN I V, COLPITTS B G, et al. A compact permanent magnet array with a remote homogeneous field[J]. *Journal of Magnetic Resonance*, 2007, 186(1): 100–104.

[11] DANIELI E, PERLO J, BLUMICH B, et al. Small magnets for portable NMR spectrometers[J]. *Angew. Chem. Int. Ed.*, 2010, 49(24): 4 133–4 135.

[12] MORESI G, MAGIN R. Miniature permanent magnet for Table-top NMR[J]. *Concepts in Magnetic Resonance Part B: Magnetic Resonance Engineering*, 2003, 19B(1): 35–43.

[13] DEMAS V, HERBERG J L, MALBA V, et al. Portable, low-cost NMR with laser-lathe lithography produced microcoils[J]. *Journal of Magnetic Resonance*, 2007, 189(1): 121–129.

[14] VISKARI P J, LANDERS J P. Unconventional detection methods for microfluidic devices[J]. *Electrophoresis*, 2006, 27(9): 1 797–1 810.

[15] HOULT D I, RICHARDS R E. The signal-to-noise ratio of the nuclear magnetic resonance experiment[J]. *Journal of Magnetic Resonance*, 1976, 24(1): 71–85.

[16] DEAN L O, TIMOTHY L P, ANDREW G W, et al. High-resolution microcoil ^{1}H-NMR for mass-limited, nanoliter-volume samples[J]. *Science*, 1995, 270(5 244): 1 967–1 970.

[17] WENSINK H, HERMES D C, VAN DEN BERG A. High signal to noise ratio in low field NMR on chip, simulations and experimental results[C]//*IEEE International Conference on Micro Electro Mechanical Systems*, Maastricht, Netherlands, January 25–29, 2004: 407–410.

[18] LU Rongsheng, WU Weiping, NI Zhonghua. Development of micro-permanent magnet magnetic circuit for nuclear magnetic resonance microscopy chip[J]. *Journal of Southeast University (Natural Science Edition)*, 2011, 41(3): 533–537. (in Chinese)

[19] WU Haicheng. *Research on MRI magnet-system with CAD method*[D]. Hefei: University of Science and Technology of China, 2007. (in Chinese)

Biographical notes

LU Rongsheng, born in 1985, is currently a PhD candidate at *School of Mechanical Engineering, Southeast University, China*. He received his bachelor degree on mechanical manufacture and automation from *Chongqing University, China*, in 2007. His research interests include miniature magnetic resonance instruments and biomedical instruments.
Tel: +86-13236538320; E-mail: lrs@seu.edu.cn

YI Hong, born in 1963, is currently director of *Jiangsu Key Laboratory for Design and Manufacture of Micro-Nano Biomedical Instruments*, president of *Southeast University, China*, a professor and a PhD candidate supervisor at *School of Mechanical Engineering, Southeast University, China*. He received his PhD degree from *Tsinghua University, China*, in 1990. His main research interests include advanced manufacturing technology, theory, design and manufacture of micro-nano-electronic mechanical systems.
Tel: +86-25-83792317; E-mail: yihong@seu.edu.cn

WU Weiping, born in 1985, is currently a PhD candidate at *School of Mechanical Engineering, Southeast University, China*. He received his bachelor degree in mechanical engineering from *Anhui University of Science and Technology, China*, in 2006 and master degree in mechatronic engineering from *Hefei University of Technology, China*, in 2009. His research interests include miniature magnetic resonance instruments and biomedical instruments.
Tel: +86-15951753276; E-mail: 230099030@seu.edu.cn

NI Zhonghua, born in 1967, is currently deputy director of *Jiangsu Key Laboratory for Design and Manufacture of Micro-Nano Biomedical Instruments*, a professor and a PhD candidate supervisor at *School of Mechanical Engineering, Southeast University, China*. He received his PhD degree from *Southeast University, China*, in 2001. His main research interests include mechanical engineering, MEMS, biomedical instruments and microfluid chip.
Tel: +86-13912960262; E-mail: nzh2003@seu.edu.cn